

## Article

# Fatigue Prediction Model and Stiffness Modulus for Semi-Flexible Pavement Surfacing Using Irradiated Waste Polyethylene Terephthalate-Based Cement Grouts

Muhammad Imran Khan <sup>1,2,\*</sup>, Muslich Hartadi Sutanto <sup>2</sup>, Shabir Hussain Khahro <sup>3,\*</sup>, Salah E. Zoorob <sup>4</sup>, Nur Izzi Md. Yusoff <sup>5</sup>, Abdalnaser M. Al-Sabaei <sup>2</sup> and Yasir Javed <sup>6</sup>

<sup>1</sup> Department of Transportation & Geotechnical Engineering, MCE, Risalpur Campus, National University of Sciences and Technology (NUST), Islamabad 44000, Pakistan

<sup>2</sup> Department of Civil & Environmental Engineering, Universiti Teknologi PETRONAS, Seri Iskandar 32610, Malaysia

<sup>3</sup> Department of Engineering Management, College of Engineering, Prince Sultan University, Riyadh 11586, Saudi Arabia

<sup>4</sup> Construction and Building Materials Program, Kuwait Institute for Scientific Research, Safat 13109, Kuwait

<sup>5</sup> Department of Civil Engineering, Universiti Kebangsaan Malaysia, Bangi 43600, Malaysia

<sup>6</sup> College of Computers and Information Sciences, Prince Sultan University, Riyadh 11586, Saudi Arabia

\* Correspondence: [engineermik@gmail.com](mailto:engineermik@gmail.com) (M.I.K.); [shkhahro@psu.edu.sa](mailto:shkhahro@psu.edu.sa) (S.H.K.)

**Abstract:** Semi-flexible pavement surfacing, or grouted macadam, is an alternative to conventional flexible and rigid pavement. It is constructed by injecting cementitious grout into the voids of an open-graded asphalt surfacing. The cement used in cementitious grouts has adverse environmental effects because of the carbon dioxide emission in cement production. The objective of this study was to investigate the potential of using irradiated waste polyethylene terephthalate (PET) and fly ash (FA) as a (partial) cement replacement in cementitious grouts for semi-flexible pavement surfacing. This study sought to assess the stiffness modulus and fatigue properties of the semi-flexible specimens prepared with control grout, regular PET (2.57% PET + 10% FA) and irradiated PET (4.75% PET + 10% FA)-based grouts and compares the stiffness modulus and fatigue properties of semi-flexible specimens with the conventional hot mix asphalt (HMA) concrete. The semi-flexible surfacing specimens showed superior performance, higher stiffness modulus, and better fatigue life than the hot mix asphalt. The difference in fatigue cycles was apparent at lower stress ratios of 25 and 30%. The semi-flexible pavement mixtures exceeded 100,000 cycles at the lowest stress ratio of 25%, while the HMA fatigue cycles were less than 100,000 cycles. Furthermore, the semi-flexible specimen with irradiated PET (which contain a higher amount of waste PET than the regular PET) showed similar stiffness modulus and fatigue life as the specimens with regular PET and control grout. The irradiation technique offers a sustainable solution for recycling higher amounts of waste PET in highway materials for semi-flexible pavement surfacing.

**Keywords:** semi-flexible surfacing; stiffness modulus; fatigue prediction model; irradiated PET; waste recycling; sustainability



**Citation:** Khan, M.I.; Sutanto, M.H.; Khahro, S.H.; Zoorob, S.E.; Md. Yusoff, N.I.; Al-Sabaei, A.M.; Javed, Y. Fatigue Prediction Model and Stiffness Modulus for Semi-Flexible Pavement Surfacing Using Irradiated Waste Polyethylene Terephthalate-Based Cement Grouts. *Coatings* **2023**, *13*, 76. <https://doi.org/10.3390/coatings13010076>

Academic Editor: Guangqing Yang

Received: 23 November 2022

Revised: 22 December 2022

Accepted: 28 December 2022

Published: 31 December 2022



**Copyright:** © 2022 by the authors. Licensee MDPI, Basel, Switzerland. This article is an open access article distributed under the terms and conditions of the Creative Commons Attribution (CC BY) license (<https://creativecommons.org/licenses/by/4.0/>).

## 1. Introduction

The semi-flexible pavement surface is a new hybrid pavement surface constructed by pouring highly flowable cementitious grout into the voids of compacted porous asphalt mixture. The typical voids of open-graded asphalt mixture designed for semi-flexible pavement surfaces range between 25–35% [1,2]. These pavements have the combined advantages of conventionally flexible and rigid pavements for rutting- and moisture-related damage, joint-free pavement, resistance to fuel spillage, and can be opened to traffic within 24 h [3]. However, the overall performance of semi-flexible pavement is

a function of aggregate type and gradation, the composition of cement grout, material stiffness properties, and testing conditions [4].

Semi-flexible pavements have different stiffness and fatigue properties from conventional flexible and rigid pavements. Setyawan (2003) investigated the effect of different types of cement grouts and varying temperatures on the stiffness properties of grouted macadam. They used limestone to produce porous asphalt and poured the asphalt with four grouts, ordinary Portland cement, OPC (control), silica fume (SF), fly ash and silica fume (FA + SF), and pozzolanic-based cement grouts. The grout type was found to have minimal effect on the indirect tensile stiffness modulus (ITSM) of grouted macadam after 28 days of curing. However, the temperature affected the stiffness modulus, where higher temperatures reduced the stiffness modulus and vice-versa [5]. van de Ven and Molenaar (2004) observed similar behavior in grouted macadam [6]. They found that temperature and loading frequency significantly influenced the stiffness modulus of grouted macadam. The results showed that the stiffness modulus of grouted macadam was more similar to conventional asphalt concrete than cement concrete. However, the fatigue testing showed that the grouted macadam was not significantly affected by testing temperature and showed similar fatigue behavior as the cement concrete [6]. Similarly, Oliveria (2006) has shown that the fatigue lines at different temperatures were very close to each other, indicating that temperature variation has minimal effect on grouted macadam's fatigue properties [7].

Semi-flexible pavement surfaces (grouted macadam) are limited to road sections for heavy loads, slow traffic, and fuel-resistant surfaces. The locations suitable for semi-flexible pavement surface include road junctions, toll plazas, gas stations, loading bays, bus stops, terminal areas, airport aprons, and fueling areas. Because semi-flexible pavements are constructed for heavy load conditions, the fatigue life can be predicted using the stress ratios concept. Most research on semi-flexible pavement mixtures established the relationship between the stress level (or stress ratio) and the number of cycles to fatigue failure [8–10]. The stiffness modulus of semi-flexible pavement mixtures is much higher than that of conventional asphalt mixtures. Therefore, a pre-determined constant strain level for both mixtures may not be suitable for comparing their fatigue lives [11]. However, the stress ratio is appropriate for determining fatigue life. Previous studies on semi-flexible pavement materials determined the stress ratios by taking a percentage level of 10 to 70% of the material's maximum indirect tensile strength [8–10].

The composition of the grouting material for semi-flexible pavement surfaces determines their performance. The composition of cement grouts may include but is not limited to cement, water, superplasticizer, sand, and fly ash (and/or other supplementary cementing materials) [12]. The cement grouts for filling the voids of open-graded asphalt mixtures must have high flowability, which is achieved by adding a superplasticizer at a relatively low w/c ratio [8,13]. Furthermore, the mechanical properties of cement grouts can be improved by adding pozzolanic binding materials such as fly ash and silica fume [14].

Cement manufacturing for the construction industries emits high amounts of greenhouse gases and is the third-largest source of carbon dioxide (CO<sub>2</sub>) emission into the environment [15,16]. Using waste materials, byproducts, and mineral admixtures in cementing materials ensures sustainability, enhanced performance, and cost-effectiveness [17,18]. Recycling municipal wastes (such as crumb rubber, glass, plastic, and wood) and industrial wastes (such as fly ash, silica fume, and ground granulated blast slag (GGBS)) utilized to replace cement and fine and coarse aggregates can preserve the ecosystem by reducing the utilization of natural resources and provide economic benefits to the construction industry in terms of cost-effectiveness and enhanced concrete properties [19,20]. FA has been widely used in concrete as a replacement of cement with promising results in improving workability and compressive strength, as well as receiving environmental benefits [15]. However, high volume FA causes reduction in compressive strength of concrete which can be improved by adding metakaolin [21]. Incorporating waste materials/byproducts in cement mortars and concrete as a replacement for cement or other natural resources (for example, sand and aggregates) reduces carbon footprint. Researchers have investigated the

feasibility of using different materials, such as using waste steel slag as a coarse aggregate, in concrete materials and predicted the electrical resistivity-compressive strength of concrete [22] and the effects of waste slag smelting on the compressive concrete strength [23], the outcome of replacing fine aggregate with waste PET [24], cement grout modified with polycarboxylate ether-based polymer [25], and the effect of GGBS and ferrous on current flow and compressive strength of concrete [26]. These modifiers/admixtures can enhance cement materials' physical and strength properties.

Researchers have investigated the effects of recycling waste PET in cement concrete manufacturing and its impacts on the strength properties by using waste plastic as fiber or fine and coarse aggregate replacement in concrete mixtures [27]. Some researchers used waste PET as an aggregate replacement to produce lightweight concrete elements [28,29]. One study showed that using recycled PET as a fiber in concrete mixture resulted in higher concrete tensile strength and crack resistance [30,31] but reduced the compressive strength significantly [32–35]. Even though incorporating PET in concrete has many benefits, it also results in a lower compressive strength. Therefore, it is essential to employ alternative procedures, such as irradiation, when recycling waste PET in cement mortar/grouts or concrete.

This study fabricated semi-flexible specimens using cement grouts containing irradiated and regular waste PET and FA as a partial cement replacement. Because of the dearth of information on the fatigue life of semi-flexible pavement surfacing, this study investigated the fatigue life of semi-flexible pavement materials through a comprehensive experimental program. The study evaluated fatigue life by establishing the relationship between stress level (kPa) and the number of cycles to fatigue failure and stress ratio (%) and the number of cycles to fatigue failure. The study performed the indirect tensile stiffness modulus test (ITMS) and indirect tensile fatigue test (ITFT) on the cylindrical specimens at varying temperatures and loadings and compared the ITMS and ITFT results with those for conventional HMA specimens. The study then developed fatigue prediction models and compared the fatigue results with those in the literature to determine the fatigue behavior of semi-flexible pavement.

## 2. Materials and Methods

### 2.1. Gamma Irradiated Waste PET

The waste PET in powder form was sourced from a recycling factory. A sufficient quantity of PET powder was irradiated with gamma rays at a dose of 100 kGy, which caused cross-linking and chain scission that increased the salinity of the PET. These changes increased the strength properties of the cement mortar and concrete [36–41]. This study used the irradiated PET in the grouts to observe their performance compared to the regular PET.

### 2.2. Cement Grouting Materials

The grouting material consists of cement, regular and irradiated waste PET powder, and fly ash. This study determined and optimized the grout composition using a response surface methodology from previous research [42]. Table 1 presents the grout compositions and their properties. The preparation of the cement grout followed the ASTM C305 standard for semi-flexible pavement mixtures and used the 0.35 w/c ratio and 1.0% superplasticizer dose for all grouts based on the author's previous research [42]. The control grout is the base cement grout for semi-flexible pavement mixtures.

**Table 1.** Composition of the pre-designed grouts and their properties.

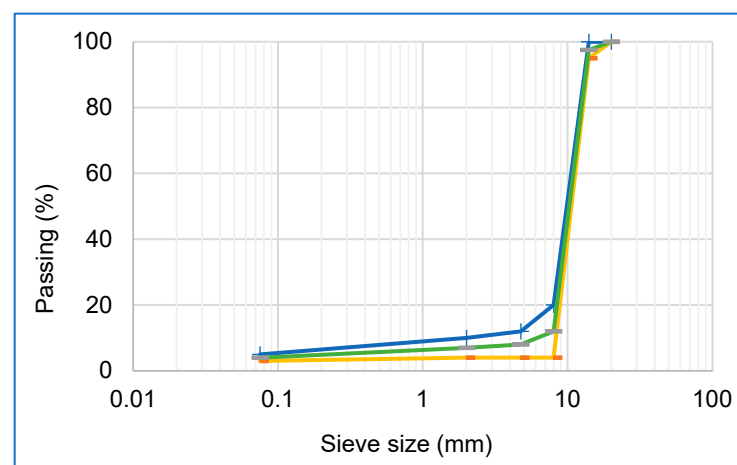
No.	Type of Grout (Symbol)	Composition of the Cement Grout	Flow Value (s)	Compressive Strength (MPa)		
				1-Day	7-Day	28-Day
1	Control grout (CN)	Cement (100%)	12.6	30.17	40.06	56.83
2	Regular PET-based grout (RP)	Cement (87.43%), RP (2.57%), Fly Ash (10%)	11.0	22.27	46.6	66.4
3	Irradiated PET-based grout (IrP)	Cement (85.25%), IrP (4.75%), Fly Ash (10%)	11.7	22.9	47.5	66.8

### 2.3. Mixture Preparation

#### 2.3.1. Selection and Mix Design of Open-Graded Asphalt Mixtures

Semi-flexible pavement surfaces are typically a combination of an open-graded asphalt mixture (with air voids ranging from 25 to 35%) and highly flowable cementitious grout poured and spread on the surface to penetrate the semi-flexible pavements [43]. The selected aggregates determine the performance of semi-flexible pavement mixtures, and previous studies have determined the gradation system for semi-flexible pavement surfaces [7,44].

This study used the REAM Type-I gap-graded asphalt (Figure 1), and the selected gradation followed the Road Engineering Association of Malaysia (REAM) guideline [45].

**Figure 1.** Gradation chart for type-1 REAM.

The recommended final optimum bitumen content (OBC) for semi-flexible pavement surfaces is a bitumen content of 3.50% by weight of aggregates based on the results obtained from the draindown test and air voids analysis.

#### 2.3.2. Preparation of the Semi-Flexible Pavement Specimens

The aggregates and bitumen (using the final OBC) were pre-heated and mixed in a mechanical mixer following the ASTM D6925 and poured into 305 mm × 305 mm × 50 mm slab molds and compacted slightly. The slab specimens were removed from the molds after 24 h. The slab molds containing porous asphalt mixtures were sealed at the joints with silicone glue to prevent any possible leakage of highly flowable cement grouts. The pre-designed cement grouts (CN, RP and IrP) were mixed, and the required grout quantity was poured on top of the slab specimen, vibrated, spread and levelled using a rubber scraper while constantly monitoring for leakages and the presence of air bubbles. Finally, the specimens were covered with plastic sheets.

The specimens were de-molded after 24 h and wrapped in waterproof polythene sheets for curing. The slabs were cored to extract cylinders with a  $100 \pm 10$  mm diameter. The cylinders after extraction were wrapped in a plastic sheet and left to cure for 28 days until the testing day.

#### 2.4. Indirect Tensile Stiffness Modulus (ITSM) Test

The stiffness of asphalt material is a critical input parameter for the structural design of pavement layers. The stiffness property measures the distribution of traffic load to the layers beneath. This test also ranks the bituminous mixtures based on their stiffness property. Another way to evaluate pavement structural behavior is by using the stiffness modulus [46]. This study used the dynamic servo-hydraulic Universal Testing Machine (UTM-100) to conduct the ITSM test on four mixtures, namely the semi-flexible pavement mixture with (i) control grout (SFM-CN), (ii) regular PET + FA-based grout (SFM-RP), (iii) irradiated PET + FA-based grout (SFM-IrP) and conventional HMA. All specimens were tested at 10, 25 and 40 °C following the BS EN 12697-26 standard [46], as shown in Figure 2. The samples for each mixture were tested at each temperature, and the average results were used in the analysis.

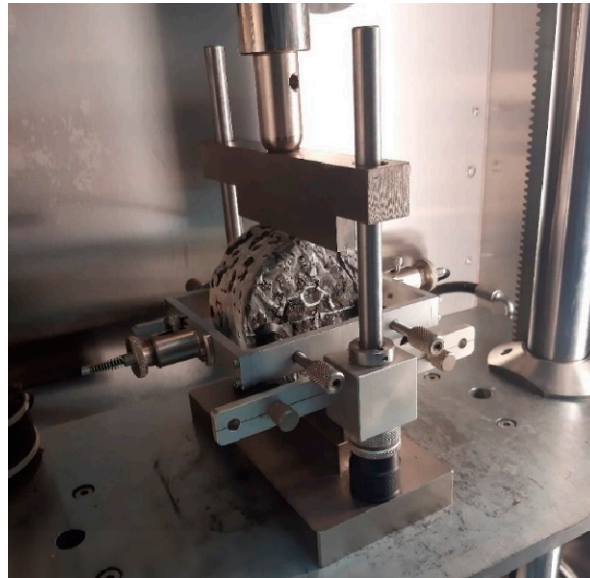


**Figure 2.** The sample position in the UTM for ITSM testing.

#### 2.5. Indirect Tensile Fatigue Test (ITFT)

This study performed the fatigue test on the cylindrical specimens, which have  $100 \pm 5$  mm diameter and are 45–50 mm high, cored from the slabs. The positioning rig was used to position and glue the deformation strips, as shown in Figure 3. It can also ascertain the position of the loading strips. The UTM-30 in the ITSM was employed to evaluate the fatigue life of semi-flexible pavement specimens. The ITFT to estimate the mixture's fatigue life was conducted at 25 °C under a stress-controlled mode and at five stress levels to obtain the best fatigue fit model. It is always appreciated to compare the fatigue life of semi-flexible with that of conventional HMA. However, because of the considerable difference in the modulus stiffness of the semi-flexible and HMA mixtures, it was inappropriate to apply the same stress levels to predict and compare the fatigue life.



**Figure 3.** Positioning rig for positioning and gluing the deformation strips on the specimen.

Therefore, this study adopted an alternative procedure using the maximum indirect tensile strength (ITS) of semi-flexible pavement mixtures and HMA mixtures. The 25, 30, 35, 40, and 45% stress ratios of the respective indirect tensile strength (ITS) values were used to perform the ITFT, which followed the BS EN 12697-24 [47]. Three specimens of each mixture and each stress ratio were tested, and the average results were used in the analysis. Figure 4 shows the setup for the ITFT. The methodology flow chart and the pictorial representation of experimental program is shown in Figures 5 and 6, respectively.

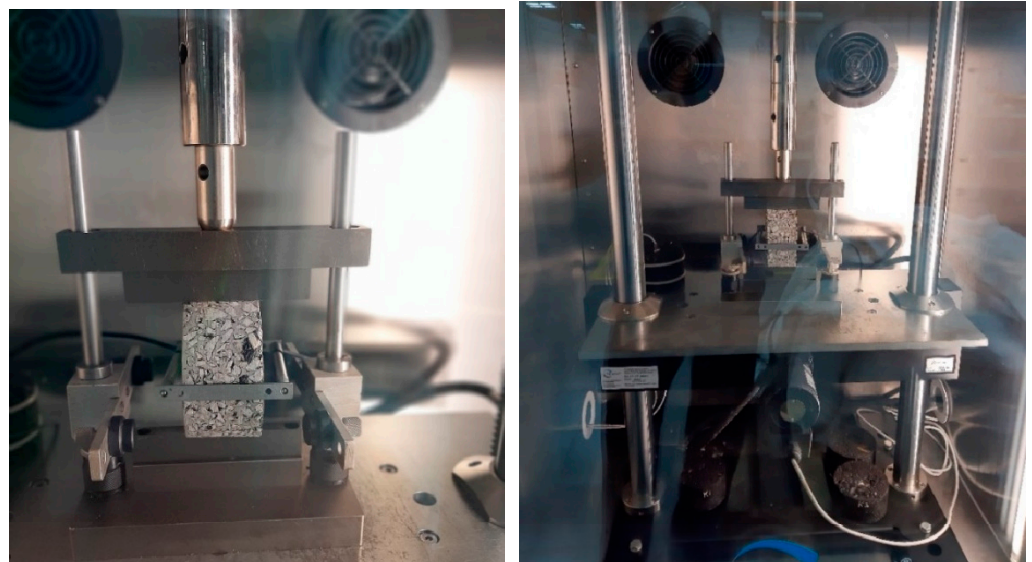


**Figure 4.** Sample position for the ITFT testing.

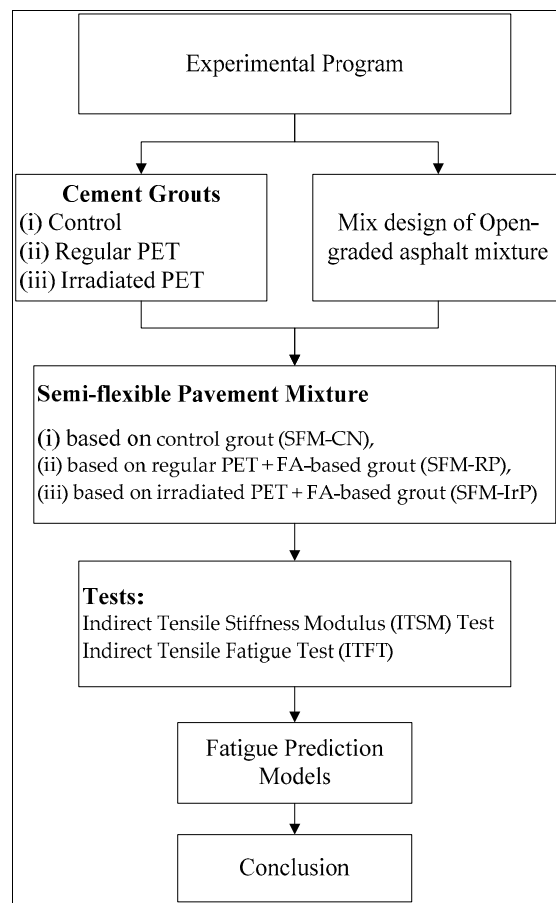


Figure 5. Methodology flow chart.

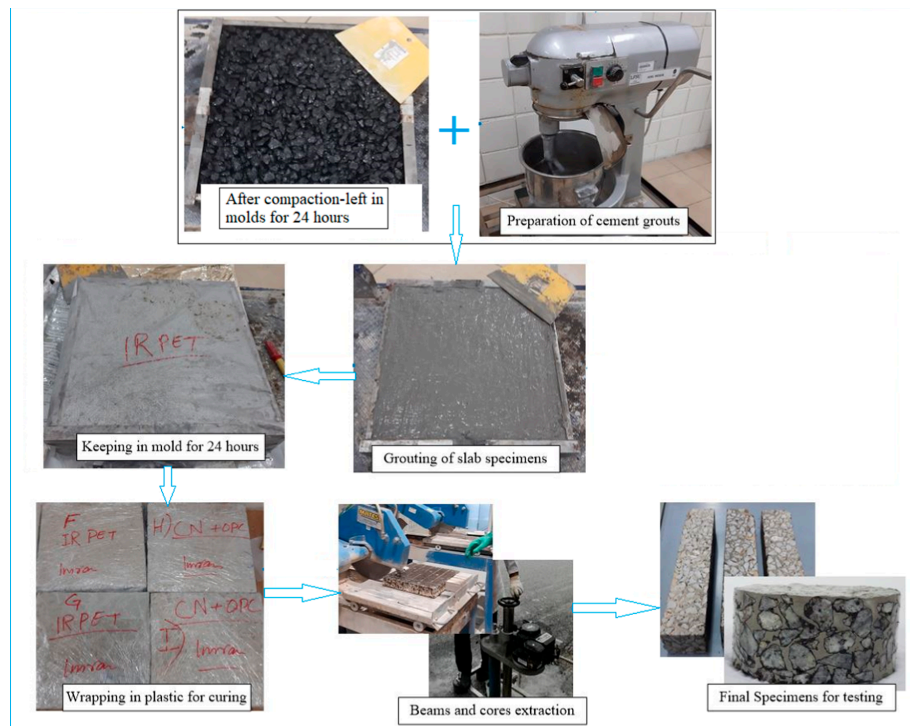


Figure 6. Pictorial representation of sample preparation [40].

### 3. Results and Discussion

#### 3.1. Stiffness Modulus of the Semi-Flexible Pavement Mixtures

The ITSM tests were carried out at varying temperatures of 10, 25, and 40 °C to determine the stiffness of the HMA and the semi-flexible specimens with different grout compositions. The test was conducted on four to five samples of each type of mixture. The average results at each temperature were used for the analysis. Figure 7 presents the average stiffness modulus of all semi-flexible pavement mixtures. The stiffness modulus of the semi-flexible pavement mixtures and HMA mixtures decreased with higher temperatures, indicating that the semi-flexible pavement mixtures are visco-elastic since the temperature increase has a considerable influence on the stiffness modulus. The lower stiffness modulus proves that the semi-flexible pavement mixtures are visco-elastic and can be directly compared with the stiffness properties of conventional HMA mixtures. Other researchers have observed a similar reduction in semi-flexible material's stiffness modulus with higher temperatures [7,43].

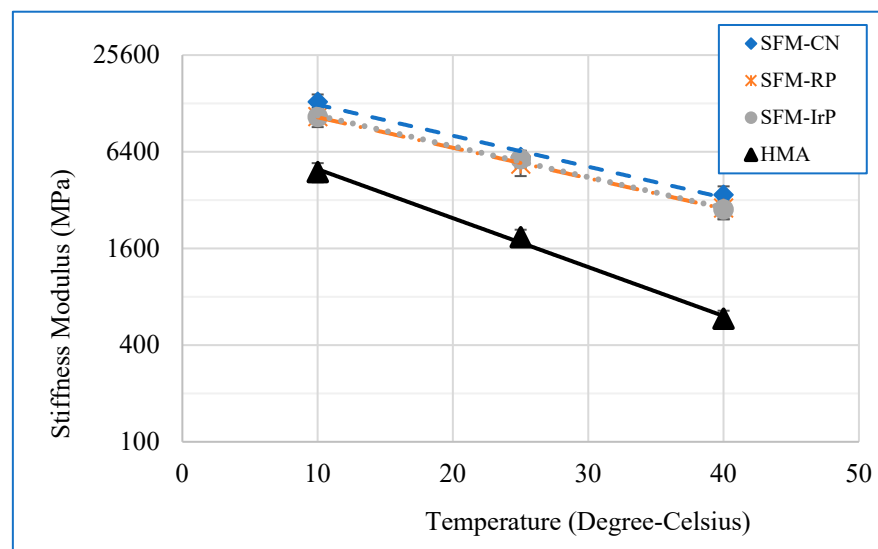
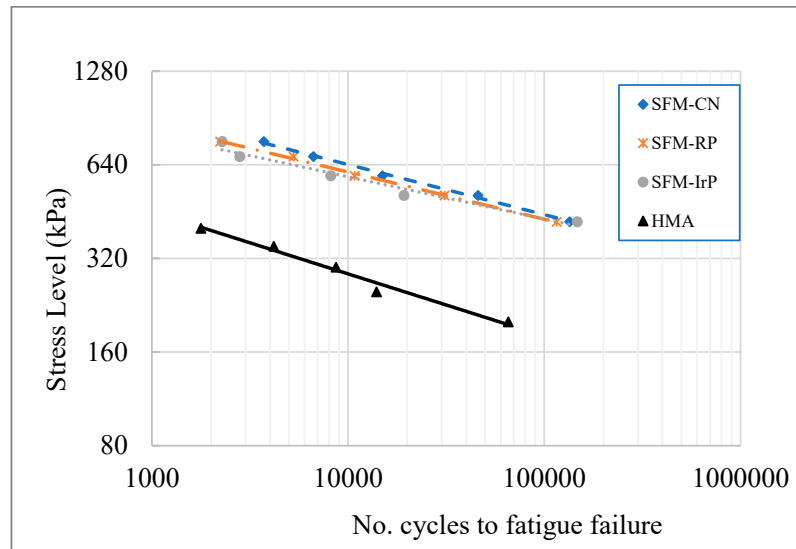


Figure 7. Stiffness modulus of semi-flexible and HMA mixture at different temperatures.

The semi-flexible pavement mixtures have a higher stiffness modulus than the conventional HMA. The regular and irradiated PET grout based semi-flexible pavement mixtures showed similar stiffness modulus results at all temperatures. The stiffness lines for SFM-RP and SFM-IrP overlap, but the SFM-CN has a slightly higher stiffness. The steeper curve of the HMA mixture indicates a significant reduction in its stiffness modulus than in the semi-flexible pavement mixtures. The stiffness of the semi-flexible surface materials means that their behavior closely resembles the behavior of bituminous material than rigid pavement material.

#### 3.2. Fatigue Life of Semi-Flexible Pavement Mixtures

The ITFT was carried out at 25 °C under controlled-stress mode to investigate the fatigue life of the semi-flexible and HMA specimens. The tests were carried out at five applied stress levels of 420, 510, 590, 680, and 760 kPa for the semi-flexible pavement mixtures, while the HMA mixtures were subjected to varying stress levels of 200, 250, 300, 350, and 400 kPa. Figure 8 shows the relationship between cycles to fatigue failure and applied stress levels (kPa).



**Figure 8.** Fatigue life at different stress ratios.

The results (Figure 8) show that the semi-flexible pavement mixtures have a slightly higher fatigue life than the HMA mixtures due to the considerable difference in their stiffness modulus. The higher lines for the fatigue life of the semi-flexible pavement mixtures indicate their higher fatigue lives. However, the fatigue lines were drawn using the stress ratios because of the significant difference in the stiffness modulus. The ITFT tests were conducted at 25, 30, 35, 40, and 45% stress ratios obtained from the ITS of the corresponding mixtures discussed in the section describing the methodology.

Figure 9 presents an alternative interpretation of the fatigue lines for each type of mixture. Figure 7 shows the fatigue lives of the semi-flexible and HMA mixtures at 25, 30, 35, 40, and 45% stress ratios, where the semi-flexible specimens reached a higher number of fatigue cycles than the HMA mixture. The difference in the fatigue lives between the semi-flexible pavement and HMA is apparent at lower stress ratios of 25% and 30%. The semi-flexible pavement mixtures exceeded the 100,000 cycles at a 25% stress ratio, while the fatigue cycles for the HMA mixture were less than 100,000 cycles. All semi-flexible pavement mixtures show higher fatigue cycles than the HMA mixture at the other stress ratios, consistent with the findings of earlier studies [9,10,48–50].

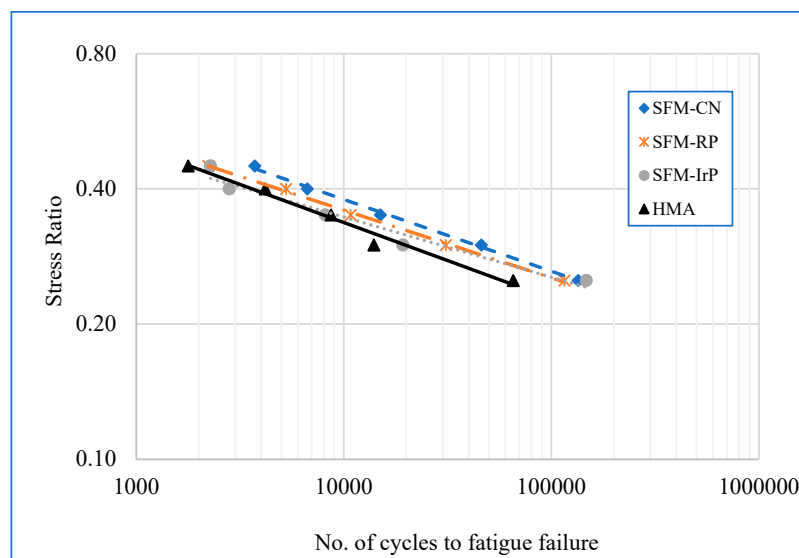


**Figure 9.** Relationship between the fatigue life and the stress ratio.

### 3.2.1. Fatigue Prediction Models for the Semi-Flexible Pavement Mixtures

Table 2 presents the fatigue models for predicting the fatigue life of the semi-flexible pavement mixtures. One method for developing the fatigue model is by establishing the relationship between the applied stress and the fatigue cycles to failure, while the other method is based on the relationship between the stress ratio and the fatigue cycles. The following fatigue model was used to predict fatigue life [7].

$$N_f = A\sigma^{-a} \quad (1)$$

where  $N_f$  is the fatigue life,  $\sigma$  is the applied stress, and  $A$  and  $a$  are the regression coefficients and obtained from experimental data.

**Table 2.** Equations developed to predict fatigue life.

Type of Mixture	Applied Stress $\sigma$ (kPa)	Stress Ratio	$N_f$ (Cycles)	Fatigue Prediction Model (Based on the Stress Levels and the Stress Ratios)	$R^2$
SFM-CN	420	0.25	134,543	$N_f = 2.31 \times 10^{21} (\sigma^{-6.19})$ $N_f = 23.44 (\sigma_r^{-6.24})$	0.99 0.99
	510	0.30	45,965		
	590	0.35	14,984		
	680	0.40	6662		
	760	0.45	3721		
SFM-RP	420	0.25	115,408	$N_f = 1.87 \times 10^{22} (\sigma^{-6.57})$ $N_f = 11.24 (\sigma_r^{-6.62})$	0.99 0.99
	510	0.30	30,980		
	590	0.35	10,776		
	680	0.40	5269		
	760	0.45	2225		
SFM-IrP	420	0.25	147,366	$N_f = 4.53 \times 10^{23} (\sigma^{-7.10})$ $N_f = 5.18 (\sigma_r^{-7.14})$	0.96 0.98
	510	0.30	19,248		
	590	0.35	8150		
	680	0.40	2804		
	760	0.45	2277		
HMA	200	0.25	65,461	$N_f = 1.07 \times 10^{16} (\sigma^{-4.90})$ $N_f = 18.59 (\sigma_r^{-5.77})$	0.98 0.80
	250	0.30	13,951		
	300	0.35	8674		
	350	0.40	4181		
	400	0.45	1778		

The  $A$  and  $a$  coefficients in the fatigue prediction equation were determined from the regression analysis. The results are presented in Table 2. The coefficient of determination ( $R^2$ ) describes the relationship between fatigue life and applied stress. Table 2 shows a higher  $R^2$  for all models, indicating a significant relationship between the applied stress and the fatigue life.

A better way to correlate the fatigue lives of mixtures is by considering the common stress ratios for the semi-flexible and HMA mixtures. Equation (2) is the fatigue life prediction model that uses the stress ratio.

$$N_f = B\sigma_r^{-b} \quad (2)$$

where  $N_f$  is the fatigue life of the mixture,  $\sigma_r$  is the stress ratio in percentage, and  $B$  and  $b$  are the regression coefficients representing the materials properties determined from laboratory tests.

This study developed the fatigue models between the stress ratio and the corresponding number of cycles to failure. Coefficients  $A$  and  $a$  for predicting fatigue was determined from the regression analysis. The results are presented in Table 2. The coefficient of determination ( $R^2$ ) describes the correlation between fatigue life and applied stress. Table 2 shows higher  $R^2$  for all models, indicating a significant correlation between the applied stress and the fatigue life.

### 3.2.2. The Fatigue Life of the Semi-Flexible Pavement

The applications of semi-flexible pavement surfaces (grouted macadam) are limited to road sections for heavy loads, slow traffic, and fuel-resistant surfaces. The semi-flexible pavement surface is typically constructed at road junctions, toll plazas, gas stations, loading bays, bus stops, terminal areas, airport aprons, and fueling areas. It is crucial to predict the fatigue life using the stress ratios for the semi-flexible pavements for heavy load conditions. Most research on semi-flexible pavement mixtures determined the relationship between the stress level (or stress ratio) and fatigue life [8–10]. The stiffness modulus of a semi-flexible pavement mixture is much higher than that of conventional asphalt mixtures. Therefore, it may not be appropriate to use a pre-determined constant strain level to compare the fatigue life of both mixtures [11].

Additionally, the stress ratio is also appropriate for investigating fatigue life. Previous studies on semi-flexible pavement materials used varying stress ratios of 10 to 70% percentages of the material's maximum indirect tensile strength [8–10]. The justification for using stress ratio for evaluating the fatigue lives of semi-flexible pavement mixtures from various literature is discussed as follows.

Sunil et al. (2020) evaluated the fatigue life of a semi-flexible pavement mixture at varying stress ratios [9] and predicted the fatigue life by establishing the relationship between fatigue cycles and stress ratios. They concluded that the ASTM gradation exhibit better fatigue life at 10, 20 and 30% stress ratios. It is worth noting that the stress ratios for the fatigue test were determined from the ITS test of the materials [9]. Another study investigated the fatigue life of semi-flexible pavement mixtures at 30, 50, and 70% stress ratios and compared the results with that of asphalt concrete. The researchers drew the fatigue curves between the number of cycles to fatigue failure and stress ratios and concluded that the grouted open-graded asphalt concretes (semi-flexible pavement mixtures) have better fatigue life than the asphalt concrete [10].

Wang et al. (2018) conducted an ITFT on semi-flexible specimens in a stress-controlled mode. They used the 20, 30 and 40% stress ratios of the indirect tensile strength of the materials to evaluate the fatigue life of carboxyl latex-modified semi-flexible pavement mixtures [48]. They also used the relationship between fatigue cycles and stress ratios to perform the regression analysis and predict the fatigue lives of semi-flexible pavement mixtures. Hou et al. (2016) conducted a beam fatigue test on semi-flexible beam specimens in a stress-controlled mode at 30%, 40%, and 50% stress ratios to investigate fatigue lives and found that the grouted macadam (semi-flexible pavement mixture) has a higher fatigue life than the dense-graded asphalt concrete [49]. Similarly, Chong et al. (2012) [50] performed a fatigue test at five stress ratios (20, 30, 40, 50, and 60%) in a stress-controlled mode on beam specimens and compared the fatigue lives of the different semi-flexible materials. They concluded that it is possible to improve the fatigue life of the semi-flexible beam specimens by using bitumen emulsion in the cement grouts [50].

These studies show that semi-flexible pavement mixtures have a higher fatigue life than dense-graded asphalt mixtures. The present study obtained a similar result, where the semi-flexible pavement mixtures exhibit higher fatigue lives (Figures 6 and 7) than the HMA.

### 3.2.3. Permanent Deformation Versus Fatigue Life

This study evaluated the fatigue failure mechanisms in semi-flexible and HMA mixtures by establishing the relationship between the cumulative deformation and the number of cycles to fatigue failure at different stress ratios, as shown in Figures 10–13. The material went through three phases before failing. Phase 1 is a very short and rapid displacement phase where the specimens underwent some compaction under repetitive loading. Phase 2 is the elastic zone with a constant deformation rate. This phase is larger than the two other phases, and the samples are usually stable. In Phase 3, the mixture is unstable, where a slight increase in the loading cycles causes a significant deformation, and the materials are in a plastic state [51,52]. Cracks appeared on the specimen surface as they entered Phase 3, which caused a complete rupture, as shown in Figure 10.

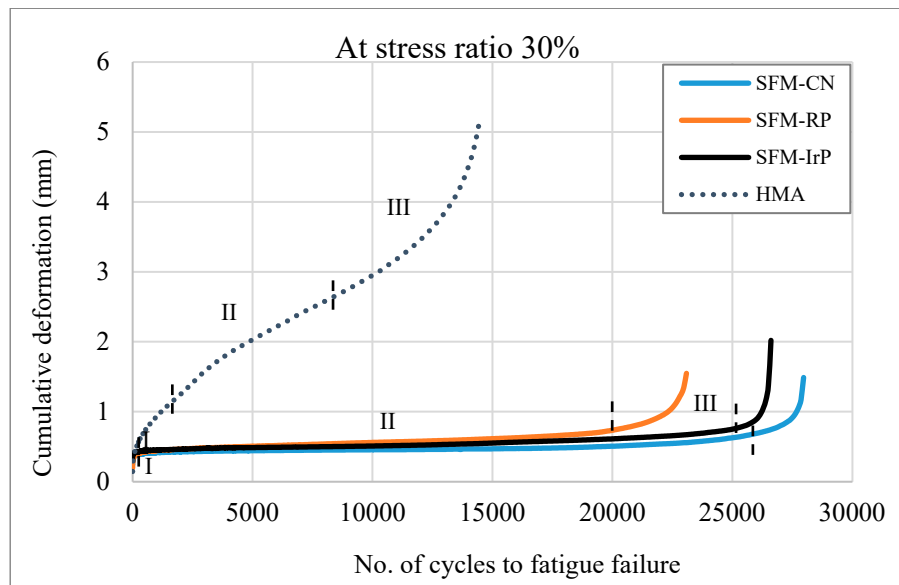


Figure 10. Number of fatigue cycles vs cumulative deformation at 30% stress ratio.

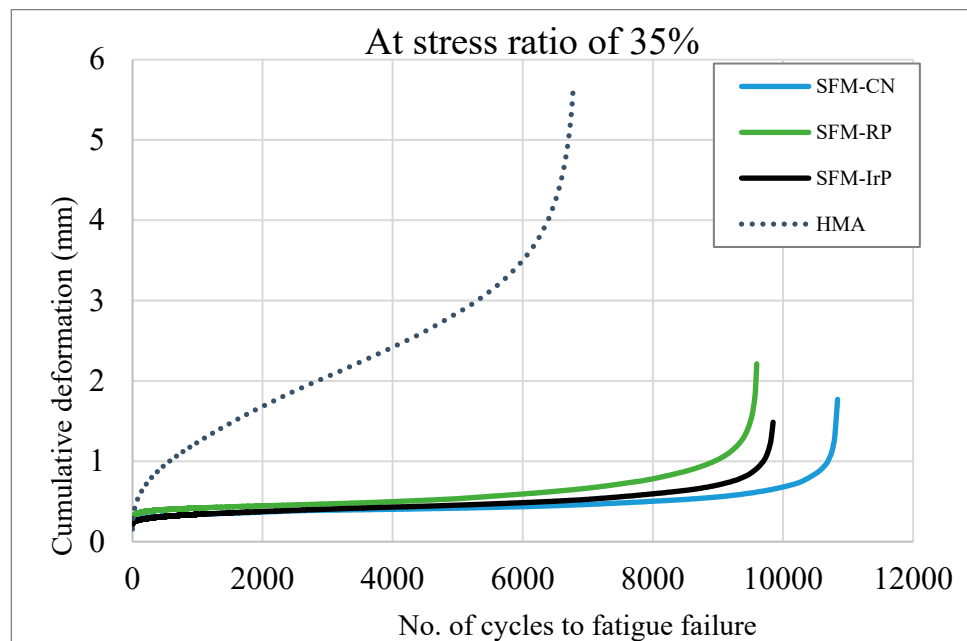


Figure 11. Number of fatigue cycles vs cumulative deformation at 35% stress ratio.

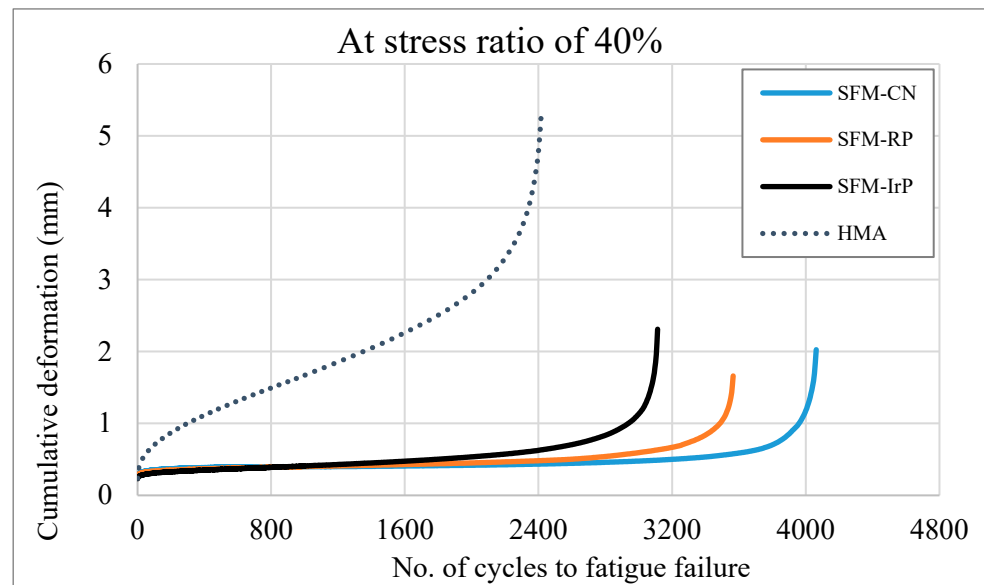


Figure 12. Number of fatigue cycles vs cumulative deformation at 40% stress ratio.

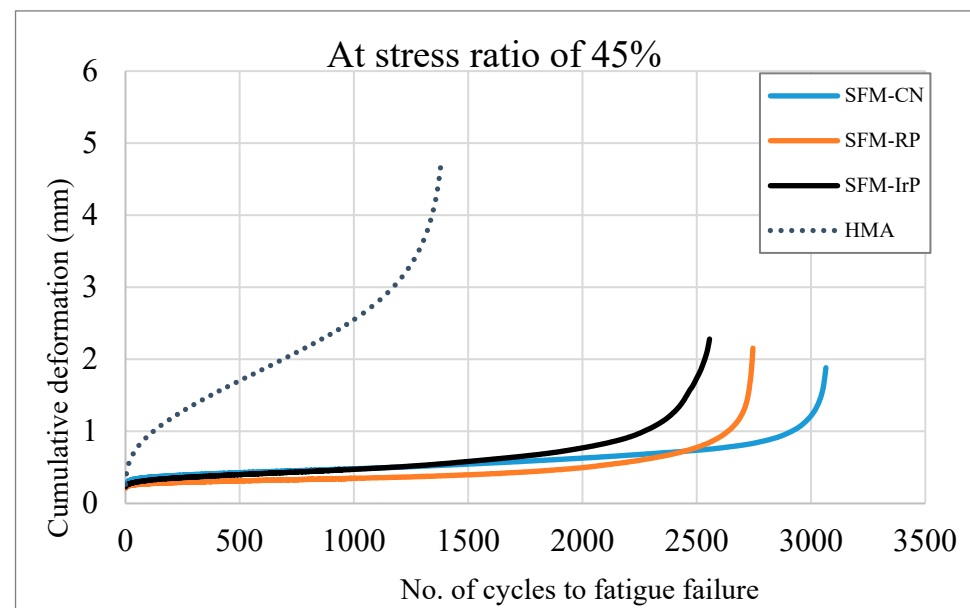


Figure 13. The relationship between cumulative deformation and the number of cycles to fatigue failure at a 45% stress ratio.

Phase 1 for the semi-flexible pavement mixture is shorter than for the HMA, possibly due to the rigid nature of the cementitious grouts. Figures 10–13 shows that, compared to the conventional HMA, all semi-flexible pavement mixtures remain in the plastic zone (Phase 2) for an extended period with minimal deformation. However, after entering Phase 3, the semi-flexible pavement mixtures underwent an abrupt and significant increase in deformation with a slight increase in fatigue cycles, causing a sudden specimen failure due to the higher stiffness modulus of semi-flexible pavement mixtures. The conventional HMA underwent complete failure after more fatigue cycles and higher deformation.

#### 4. Conclusions

This study investigated the stiffness and fatigue properties of semi-flexible pavement material with different cement grouts by considering the effects of varying temperatures on stiffness modulus and varying loading on fatigue properties. It developed fatigue models

for predicting the fatigue life of semi-flexible materials. Based on the study results, the authors draw the following conclusions.

1. The increase in temperature caused a considerable reduction in the stiffness modulus of semi-flexible and HMA mixtures. The change in the stiffness modulus of the semi-flexible pavement mixture with temperature indicates that the semi-flexible pavement mixtures have a viscoelastic behavior, which allows for a direct comparison of the semi-flexible pavement mixtures with the stiffness properties of conventional HMA mixtures. However, the cement grout in the semi-flexible pavement mixtures gave them a higher stiffness than the HMA mixture.
2. Analysis of the fatigue life based on the stress ratio revealed that the semi-flexible pavement mixtures have higher fatigue life than the conventional HMA. The overlapping of the fatigue lines of the semi-flexible pavement mixtures (control, regular PET and irradiated PET) indicates that all mixtures have a similar fatigue resistance.
3. The fatigue prediction models are based on existing fatigue models and regression analysis. The fatigue models are well-fitted, and the correlation ( $R^2 > 0.90$ ) between the number of cycles to fatigue failure and applied stress or initial strain was significant.
4. The semi-flexible pavement mixture with regular PET (SFM-RP) and irradiated PET (SFM-IrP) have similar fatigue results, indicating that it is possible to use a higher percentage of waste irradiated PET (4.75%) than the regular waste PET (2.57%).

**Author Contributions:** Conceptualization, M.I.K.; methodology, M.H.S., software, Y.J.; validation, M.I.K., A.M.A.-S. and S.H.K.; formal analysis, M.H.S. and S.E.Z.; writing—original draft preparation, M.I.K., A.M.A.-S. and S.E.Z.; writing—review and editing, S.H.K. and N.I.M.Y.; visualization. All authors have read and agreed to the published version of the manuscript.

**Funding:** This research received no external funding.

**Institutional Review Board Statement:** Not applicable.

**Informed Consent Statement:** Not applicable.

**Data Availability Statement:** Not applicable.

**Acknowledgments:** The authors thank Universiti Teknologi PETRONAS (UTP), Malaysia and the National University of Sciences and Technology (NUST), Islamabad, Pakistan, for being supportive for this study. The authors are grateful to Prince Sultan University (PSU), Riyadh, Saudi Arabia, for paying the Article Processing Charges (APC) and scholarly support for the publication of this paper.

**Conflicts of Interest:** The authors declare no conflict of interest.

## References

1. Oliveira, J.R.; Pais, J.C.; Thom, N.H.; Zoorob, S.E. A Study of the Fatigue Properties of Grouted Macadams. *Int. J. Pavements* **2007**, *6*, 112–123.
2. Pratelli, C.; Betti, G.; Giuffrè, T.; Marradi, A. Preliminary In-Situ Evaluation of an Innovative, Semi-Flexible Pavement Wearing Course Mixture Using Fast Falling Weight Deflectometer. *Materials* **2018**, *11*, 611. [[CrossRef](#)] [[PubMed](#)]
3. Khan, M.I.; Huat, H.Y.; Dun, M.H.b.M.; Sutanto, M.H.; Jarghouyeh, E.N.; Zoorob, S.E. Effect of Irradiated and Non-Irradiated Waste PET Based Cementitious Grouts on Flexural Strength of Semi-Flexible Pavement. *Materials* **2019**, *12*, 4133. [[CrossRef](#)] [[PubMed](#)]
4. Hamzani; Munirwansyah; Hasan, M.; Sugiarto, S. Determining the properties of semi-flexible pavement using waste tire rubber powder and natural zeolite. *Constr. Build. Mater.* **2021**, *266*, 121199. [[CrossRef](#)]
5. Hassan, K.; Setyawan, A.; Zoorob, S. Effect of cementitious grouts on the properties of semi-flexible bituminous pavements. In Proceedings of the 4th European Symposium on Performance of Bituminous and Hydraulic Materials in Pavements, Bitmat4, Nottingham, UK, 11–12 April 2002; Routledge: London, UK, 2002; pp. 113–120.
6. Van de Ven, M.; Molenaar, A. Mechanical Characterization of Combi-layer. *Asph. Paving Technol.* **2004**, *73*, 1–22.
7. Oliveira, J.R. Grouted Macadam: Material Characterisation for Pavement Design. Ph.D. Thesis, University of Nottingham, Nottingham, UK, 2006.
8. Wang, Y.J.; Guo, C.Y.; Tian, Y.F.; Wang, J.J. Design of Mix Proportion of Cement Mortar with High-Performance Composite Semi-Flexible Pavement. *Adv. Mater. Res.* **2013**, *641–642*, 342–345. [[CrossRef](#)]

9. Sunil, S.; Varuna, M.; Nagakumar, M.S. Performance evaluation of semi rigid pavement mix. *Mater. Today Proc.* **2020**, *46*, 4771–4775. [[CrossRef](#)]
10. Zhong, K.; Sun, M.; Zhang, M.; Qin, Y.; Li, Y. Interfacial and mechanical performance of grouted open-graded asphalt concrete with latex modified cement mortar. *Constr. Build. Mater.* **2020**, *234*, 117394. [[CrossRef](#)]
11. Luo, S.; Yang, X.; Zhong, K.; Yin, J. Open-graded asphalt concrete grouted by latex modified cement mortar. *Road Mater. Pavement Des.* **2018**, *21*, 61–77. [[CrossRef](#)]
12. Shukla, M.; Gottumukkala, B.; Nagabhushana, M.N.; Chandra, S.; Shaw, A.; Das, S. Design and evaluation of mechanical properties of cement grouted bituminous mixes (CGBM). *Constr. Build. Mater.* **2021**, *269*, 121805. [[CrossRef](#)]
13. Cai, J.; Pei, J.; Luo, Q.; Zhang, J.; Li, R.; Chen, X. Comprehensive service properties evaluation of composite grouting materials with high-performance cement paste for semi-flexible pavement. *Constr. Build. Mater.* **2017**, *153*, 544–556. [[CrossRef](#)]
14. Zhang, J.; Cai, J.; Pei, J.; Li, R.; Chen, X. Formulation and performance comparison of grouting materials for semi-flexible pavement. *Constr. Build. Mater.* **2016**, *115*, 582–592. [[CrossRef](#)]
15. Ondova, M.; Stevulova, N.; Estokova, A. The study of the properties of fly ash based concrete composites with various chemical admixtures. *Procedia Eng.* **2012**, *42*, 1863–1872. [[CrossRef](#)]
16. Shanks, W.; Dunant, C.F.; Drewniok, M.P.; Lupton, R.C.; Serrenho, A.; Allwood, J.M. How much cement can we do without? Lessons from cement material flows in the UK. *Resour. Conserv. Recycl.* **2019**, *141*, 441–454. [[CrossRef](#)]
17. Turanli, L.; Uzal, B.; Bektas, F. Effect of large amounts of natural pozzolan addition on properties of blended cements. *Cem. Concr. Res.* **2005**, *35*, 1106–1111. [[CrossRef](#)]
18. Elmrbet, R.; El Harfi, A.; El Youbi, M. Study of properties of fly ash cements. *Mater. Today Proc.* **2019**, *13*, 850–856. [[CrossRef](#)]
19. Siddique, R. Utilization of industrial by-products in concrete. *Procedia Eng.* **2014**, *95*, 335–347. [[CrossRef](#)]
20. Dixit, A. A study on the physical and chemical parameters of industrial by-products ashes useful in making sustainable concrete. *Mater. Today Proc.* **2021**, *43*, 42–50. [[CrossRef](#)]
21. Nie, Y.; Shi, J.; He, Z.; Zhang, B.; Peng, Y.; Lu, J. Evaluation of high-volume fly ash (HVFA) concrete modified by metakaolin: Technical, economic and environmental analysis. *Powder Technol.* **2022**, *397*, 117121. [[CrossRef](#)]
22. Shakr Piro, N.; Mohammed, A.; Hamad, S.M.; Kurda, R. Electrical Resistivity-Compressive strength predictions for normal strength concrete with waste steel slag as a coarse aggregate replacement using various analytical models. *Constr. Build. Mater.* **2022**, *327*, 127008. [[CrossRef](#)]
23. Piro, N.S.; Mohammed, A.S.; Hamad, S.M.; Kurda, R. Electrical conductivity, microstructures, chemical compositions, and systematic multivariable models to evaluate the effect of waste slag smelting (pyrometallurgical) on the compressive strength of concrete. *Environ. Sci. Pollut. Res.* **2022**, *29*, 68488–68521. [[CrossRef](#)] [[PubMed](#)]
24. Qaidi, S.; Al-Kamaki, Y.S.S.; Al-Mahaidi, R.; Mohammed, A.S.; Ahmed, H.U.; Zaid, O.; Althoey, F.; Ahmad, J.; Isleem, H.F.; Bennetts, I. Investigation of the effectiveness of CFRP strengthening of concrete made with recycled waste PET fine plastic aggregate. *PLoS ONE* **2022**, *17*, e0269664. [[CrossRef](#)] [[PubMed](#)]
25. Mahmood, W.; Mohammed, A.S.; Sihag, P.; Asteris, P.G.; Ahmed, H. Interpreting the experimental results of compressive strength of hand-mixed cement-grouted sands using various mathematical approaches. *Arch. Civ. Mech. Eng.* **2021**, *22*, 19. [[CrossRef](#)]
26. Piro, N.S.; Mohammed, A.S.; Hamad, S.M. The impact of GGBS and ferrous on the flow of electrical current and compressive strength of concrete. *Constr. Build. Mater.* **2022**, *349*, 128639. [[CrossRef](#)]
27. Alani, A.H.; Bunnori, N.M.; Noaman, A.T.; Majid, T.A. Durability performance of a novel ultra-high-performance PET green concrete (UHPPGC). *Constr. Build. Mater.* **2019**, *209*, 395–405. [[CrossRef](#)]
28. Choi, Y.W.; Moon, D.J.; Kim, Y.J.; Lachemi, M. Characteristics of mortar and concrete containing fine aggregate manufactured from recycled waste polyethylene terephthalate bottles. *Constr. Build. Mater.* **2009**, *23*, 2829–2835. [[CrossRef](#)]
29. Akçaözoglu, S.; Atiş, C.D.; Akçaözoglu, K. An investigation on the use of shredded waste PET bottles as aggregate in lightweight concrete. *Waste Manag.* **2010**, *30*, 285–290. [[CrossRef](#)]
30. Fraternali, F.; Ciancia, V.; Chechile, R.; Rizzano, G.; Feo, L.; Incarnato, L. Experimental study of the thermo-mechanical properties of recycled PET fiber-reinforced concrete. *Compos. Struct.* **2011**, *93*, 2368–2374. [[CrossRef](#)]
31. Borg, R.P.; Baldacchino, O.; Ferrara, L. Early age performance and mechanical characteristics of recycled PET fibre reinforced concrete. *Constr. Build. Mater.* **2016**, *108*, 29–47. [[CrossRef](#)]
32. Marzouk, O.Y.; Dheilly, R.M.; Queneudec, M. Valorization of post-consumer waste plastic in cementitious concrete composites. *Waste Manag.* **2007**, *27*, 310–318. [[CrossRef](#)]
33. Albano, C.; Camacho, N.; Hernández, M.; Matheus, A.; Gutiérrez, A. Influence of content and particle size of waste pet bottles on concrete behavior at different w/c ratios. *Waste Manag.* **2009**, *29*, 2707–2716. [[CrossRef](#)] [[PubMed](#)]
34. Remadnia, A.; Dheilly, R.M.; Laidoudi, B.; Quéneudec, M. Use of animal proteins as foaming agent in cementitious concrete composites manufactured with recycled PET aggregates. *Constr. Build. Mater.* **2009**, *23*, 3118–3123. [[CrossRef](#)]
35. Batayneh, M.; Marie, I.; Asi, I. Use of selected waste materials in concrete mixes. *Waste Manag.* **2007**, *27*, 1870–1876. [[CrossRef](#)] [[PubMed](#)]
36. Schaefer, C.E.; Kupwade-Patil, K.; Ortega, M.; Soriano, C.; Büyüköztürk, O.; White, A.E.; Short, M.P. Irradiated recycled plastic as a concrete additive for improved chemo-mechanical properties and lower carbon footprint. *Waste Manag.* **2018**, *71*, 426–439. [[CrossRef](#)]

37. Khan, M.I.; Sutanto, M.H.; Napiah, M.B.; Zoorob, S.E. Cementitious Grouts Containing Irradiated Waste Polyethylene Terephthalate. In *Cement Industry-Optimization, Characterization and Sustainable Application*; Saleh, H.M., Ed.; IntechOpen: London, UK, 2020.
38. Khan, M.I.; Sutanto, M.H.; Khan, K.; Iqbal, M.; Napiah, M.B.; Zoorob, S.E.; Klemeš, J.J.; Bokhari, A.; Rafiq, W. Effective use of recycled waste PET in cementitious grouts for developing sustainable semi-flexible pavement surfacing using artificial neural network (ANN). *J. Clean. Prod.* **2022**, *340*, 130840. [[CrossRef](#)]
39. Khan, M.I.; Sutanto, M.H.; Napiah, M.B.; Khan, K.; Rafiq, W. Design optimization and statistical modeling of cementitious grout containing irradiated plastic waste and silica fume using response surface methodology. *Constr. Build. Mater.* **2021**, *271*, 121504. [[CrossRef](#)]
40. Khan, M.I.; Sutanto, M.H.; Napiah, M.B.; Zoorob, S.E.; Al-Sabaei, A.M.; Rafiq, W.; Ali, M.; Memon, A.M. Investigating the mechanical properties and fuel spillage resistance of semi-flexible pavement surfacing containing irradiated waste PET based grouts. *Constr. Build. Mater.* **2021**, *304*, 124641. [[CrossRef](#)]
41. Khan, M.I.; Wen, L.S.; Sutanto, M.H.; Napiah, M.B.; Zoorob, S.E. Effect of Cement Grouts Containing Irradiated Polyethylene Terephthalate on Properties of Semi-Flexible Mixtures. *Key Eng. Mater.* **2021**, *888*, 3–8. Available online: <https://www.scientific.net/KEM.888.3> (accessed on 27 November 2022). [[CrossRef](#)]
42. Khan, M.I.; Sutanto, M.H.; Napiah, M.B.; Zoorob, S.E.; Yusoff, N.I.M.; Usman, A.; Memon, A.M. Irradiated polyethylene terephthalate and fly ash based grouts for semi-flexible pavement: Design and optimisation using response surface methodology. *Int. J. Pavement Eng.* **2020**, *23*, 2515–2530. [[CrossRef](#)]
43. Anderton, G.L. *Engineering Properties of Resin Modified Pavement (RMP) for Mechanistic Design*; Engineer Research and Development Center Vicksburg MS Geotechnical Lab: Vicksburg, MS, USA, 2000.
44. Hou, S.; Xu, T.; Huang, K. Aggregate Gradation Influence on Grouting Results and Mix Design of Asphalt Mixture Skeleton for Semi-Flexible Pavement. *J. Test. Eval.* **2017**, *45*, 591–600. [[CrossRef](#)]
45. REAM. *Road Engineering Association of Malaysia, "Specification of Semi-Rigid Wearing Course"*; Road Engineering Association of Malaysia (REAM): Selangor, Malaysia, 2007.
46. *BS-EN-12697-26; Bituminous Mixtures—Test Methods for Hot Mix Asphalt—Part 26: Stiffness*. British Standards: London, UK, 2004.
47. *BS-EN-12697-24; Bituminous Mixtures—Test Methods for Hot Mix Asphalt—Part 24: Resistance to Fatigue*. British Standards: London, UK, 2012; Volume 24.
48. Wang, D.; Liang, X.; Jiang, C.; Pan, Y. Impact analysis of Carboxyl Latex on the performance of semi-flexible pavement using warm-mix technology. *Constr. Build. Mater.* **2018**, *179*, 566–575. [[CrossRef](#)]
49. Hou, S.; Xu, T.; Huang, K. Investigation into engineering properties and strength mechanism of grouted macadam composite materials. *Int. J. Pavement Eng.* **2016**, *17*, 878–886. [[CrossRef](#)]
50. Huang, C.; Liu, J.P.; Hong, J.X.; Liu, Z.F. Improvement on the crack resistance property of semi-flexible pavement by cement-emulsified asphalt mortar. In *Key Engineering Materials*; Trans Tech Publications Ltd.: Wollerau, Switzerland, 2012; pp. 26–32.
51. Baghaee Moghaddam, T.; Karim, M.R.; Syammaun, T. Dynamic properties of stone mastic asphalt mixtures containing waste plastic bottles. *Constr. Build. Mater.* **2012**, *34*, 236–242. [[CrossRef](#)]
52. Behbahani, H.; Najafi Moghaddam Gilani, V.; Salehfard, R.; Safari, D. Evaluation of Fatigue and Rutting Behaviour of Hot Mix Asphalt Containing Rock Wool. *Int. J. Civ. Eng.* **2020**, *18*, 1293–1300. [[CrossRef](#)]

**Disclaimer/Publisher's Note:** The statements, opinions and data contained in all publications are solely those of the individual author(s) and contributor(s) and not of MDPI and/or the editor(s). MDPI and/or the editor(s) disclaim responsibility for any injury to people or property resulting from any ideas, methods, instructions or products referred to in the content.